Available online at www.sciencedirect.com

ScienceDirect

Procedia CIRP 138 (2026) 1201–1206

www.elsevier.com/locate/procedia

18th CIRP Conference on Intelligent Computation in Manufacturing Engineering

Enhancing Bioprinting Precision through Real-Time Monitoring of Stand-Off Distance: a preliminary study

Alessandro Margarita, Simone Gugliandolo, Bianca Maria Colosimo*

Department of Mechanical Engineering, Politecnico di Milano, Via La Masa, 1, 20156, Milano, Italy;

* Corresponding author. *E-mail address:* biancamaria.colosimo@polimi.it

Abstract

The rapidly evolving field of 3D bioprinting holds immense promise for tissue engineering and regenerative medicine, yet achieving high-quality structures remains challenging, making the development of monitoring techniques crucial.
This work presents a cutting-edge real-time monitoring technique in bioprinting. Through a digital microscope it is possible to accurately assess the distance between the extruder and the substrate in real-time, providing crucial data for optimizing parameters. Experiments were performed using Gelatine Alginate at different concentrations. The sensor's integration enables continuous monitoring, offering instant feedback on printing quality, enhancing overall bioprinted structure quality and moving towards automated, closed-loop control systems.

Keywords: bioprinting; zero-defect; zero-waste; insitu monitoring, additive manufacturing; Data mining.

1. Introduction

3D Bioprinting is an interdisciplinary field merging additive manufacturing, tissue engineering, and material sciences, that is gaining significant attention due to its wide-ranging applications across various sectors, embracing the medical [1], the aerospace [2-6] and also food industries [7-9]. Its potential to revolutionize regenerative medicine, pharmaceuticals, cosmetics, biological studies, and medical research highlights its versatility and promise in both scientific and industrial realms [10].

However, despite the promising prospects of 3D bioprinting, certain challenges persist, particularly regarding the reproducibility and reliability of the process. Ensuring consistent quality is essential for widespread adoption, necessitating thorough qualification of the bioprinting process.

While considerable efforts have been dedicated to ex-situ qualification, there remains a noticeable gap in real-time monitoring solutions to assess the quality of 3D bioprinted constructs during the printing process itself. Implementing in-situ monitoring is fundamental for adaptive process optimization and control, facilitating a deeper understanding of critical process features. Such advancements could lead to more efficient bioprinting, reducing resource consumption.

Although there is growing interest in monitoring bioprinting processes, existing literature primarily focuses on monitoring shape fidelity layer wise, i.e., measuring the deviation between intended and actual shapes of bioprinted constructs on the X-Y plane.

This objective can be achieved through various sensor technologies, such as optical cameras [11-14], optical

10.1016/j.procir.2026.01.207

coherence tomography (OCT) [15-16], and laser scanning [17]. Additionally, thermal video imaging has emerged as a feasible method for monitoring shape accuracy when using transparent bioinks [18]. Other studies have delved into observing droplet characteristics in inkjet bioprinting [19, 20], and tracking temperature fluctuations in all components of an extrusion bioplotter while printing thermo-responsive materials [21].

Particularly in the context of intricate and multi-layered constructs, where printing times are extended to accommodate the complexity of the design, monitoring and optimizing the stand-off distance, i.e., the distance between the extruder and the printed layer, assumes heightened significance, playing a pivotal role in determining the quality, fidelity, and functionality of bioprinted constructs.

Maintaining an optimal stand-off distance is essential for ensuring precise deposition of bioink onto the substrate. Deviations from the ideal distance can result in irregularities in layer formation, compromising structural integrity and functional performance.

In this work a new method for stand-off distance monitoring is presented. Our method entails continuous monitoring of the printing process using a high-resolution digital microscope, which enables real-time visualization and quantification of the layer thickness.

By quantifying layer thickness at different stages of bioprinting, we can elucidate the effects of prolonged printing times on construct integrity and identify potential areas for optimization.

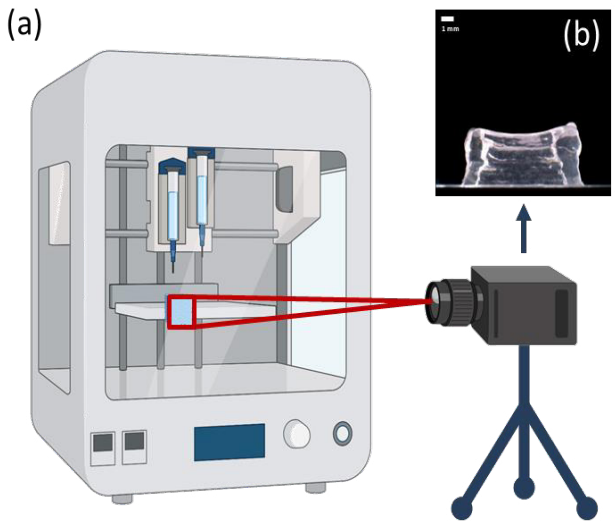

Figure 1. (a) Schematized monitoring setup. (b) Frame taken with the monitoring system.

2. Materials and Methods

2.1. Bioink Preparation

Alginate-Gelatin blends were prepared at the concentration Alg-Gel 4%-4% (w/v) (AlgGel4%). The solution was prepared from lyophilized sodium alginate and gelatin (Sigma-Aldrich, St. Louis, Missouri, USA). A volume of 15 ml of phosphate-buffered saline (PBS) was mixed with alginate and gelatin powders with a weight 0.6 g – 0.6 g. The solution was then heated up to 50 °C and stirred with a magnetic mixer for 1 hour until a homogeneous material was obtained. The final product was stored in fridge at 6 °C.

2.2. Monitoring Setup

Monitoring setup is shown in Figure 1. The recording system is made by a digital microscope (Dino-Lite Digital Microscope, Almere, The Netherland) and a height-adjustable custom support. The digital microscope was connected to a computer and videos were collected through the dedicated software DinoXcope (Dino-Lite Digital Microscope, Almere, The Netherlands). Based on DinoLite performance, every video was recorded with a fixed framerate at 45 fps, and a resolution of 1280x960 pixels. At the optimal distance for the used system, the spatial resolution is 14 µm/pixel.

A black paper sheet was placed behind the petri dish, in order to obtain a contrast with the deposited material. The petri dish was turned upside-down to obtain a close-up image of the printed object and covered on the side with black tape to avoid light reflection.

2.3. Bioprinting Process and Video Analysis

For this work, a pneumatic extrusion bioprinter (BioX, Cellink AB, Sweden) was used. Before the printing process, each biomaterial was heated up to 37 °C for 10 minutes until liquid, put in a cartridge, re-heated up to 37 °C for 5 more minutes and centrifuged at 1800 rpm for 5 minutes to remove bubbles. Finally, the cartridge was placed in a temperature-controlled printhead (Cellink AB, Sweden) to set the right temperature of the biomaterial. The material was deposited using 0.410 mm conical nozzles (22 G).

Only the perimeters of 10x4x3.7 mm parallelepipeds were printed, in order to obtain a hollow structure. Printing parameters are reported in Table 1.

A number n = 3 of replicates was printed, for a total of 24 structures. The printing process of every structure was entirely recorded, and then each sub-video was extracted using ShotCut software (MeltyTech LLC) and analysed.

Table 1. Printing parameters

Bioink	Pressure [kPa]	Speed [mm/s]	Printhead T [°C]	Printbed T [°C]	Pre-flow delay [ms]
AlgGel4%	38	9	28	10	250

Raw videos were elaborated using MATLAB (The MathWorks Inc., Natick, Massachusetts, USA).

Each frame was first cropped with a rectangular window, filtered with a custom filter for low-exposure images, and segmented using a k-means clustering method (a number of clusters n = 2, a maximum number of iterations nmax = 100, and a threshold distance between centroids in consecutive iterations of dth = 1e-4), resulting in a logical mask which was further applied to the original image.

In the processing part, the layer height value was extracted from each frame using a modified version of the algorithm in the work of Strauß et al. [11]: treating the image as a matrix, starting from the first and the last pixel of each column, a top and a bottom white pixel were found, and the height was calculated as the distance between them, and then multiplied by a conversion factor previously obtained with the calibration process:

$$height = (bottom\ px - top\ px) \times conversion\ factor$$

This approach resulted particularly useful in the case of transparent materials, since it overtook segmentation problems related to light reflections and artifacts, ignoring pixels between the two boundaries which potentially could be included in a wrong cluster. Then, an average value of height was calculated on the number of columns. In post-processing, every average height value was plotted in a height-time graph for the analysis of the height profile in time.

For the statistical analysis, Shapiro-Wilk Normality test on residuals and linear regression and filtering analyses were carried out using Curve Fitter and Signal Analyzer tools available in MATLAB (The MathWorks Inc., Natick, Massachusetts, USA).

3. Results

Firstly, height reduction over time of each single layer was studied. Each dataset was filtered with a Savitzky-Golay (SG) smooth filter, and the height reduction value was calculated as the difference between the height extracted from the first and the last frame of each video recorded, and then expressed as mean value and standard deviation between replicates. This approach was applied to all the experimental campaigns, excluding the control.

Results of the height reduction study are reported in Table 2, while a graphical representation of the overmentioned reduction is shown in Figure 2.

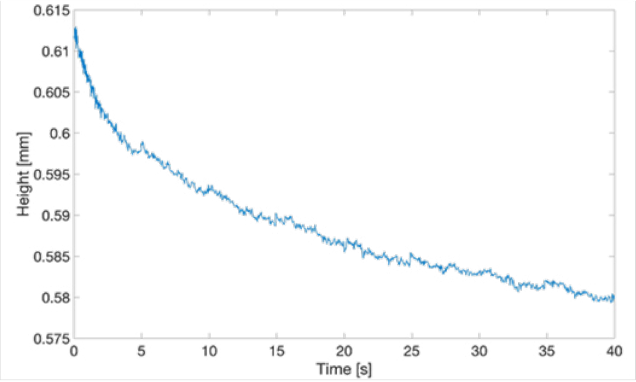

Figure 2. Example of height reduction in layer 1.

Table 2. Height reduction per each layer.

AlgGel4% Height Reduction [mm]

Time [s] ↓	Layer →	1	2	3	4	5	6	7	8	9
10		0.048 ± 0.009	0.043 ± 0.004	0.033 ± 0.003	0.023 ± 0.002	0.017 ± 0.002	0.025 ± 0.016	0.029 ± 0.003	0.042 ± 0.015	0.041 ± 0.010
20		0.055 ± 0.006	0.056 ± 0.004	0.044 ± 0.001	0.042 ± 0.004	0.036 ± 0.002	0.051 ± 0.019	0.032 ± 0.004	0.031 ± 0.015	0.041 ± 0.008
40		0.066 ± 0.004	0.063 ± 0.002	0.056 ± 0.004	0.054 ± 0.001	0.053 ± 0.003	0.051 ± 0.006	0.073 ± 0.011	0.045 ± 0.010	0.062 ± 0.004

Peer-review under responsibility of the scientific committee of the 18th CIRP Conference on Intelligent Computation in Manufacturing Engineering, 10-12 July, Gulf of Naples, Italy

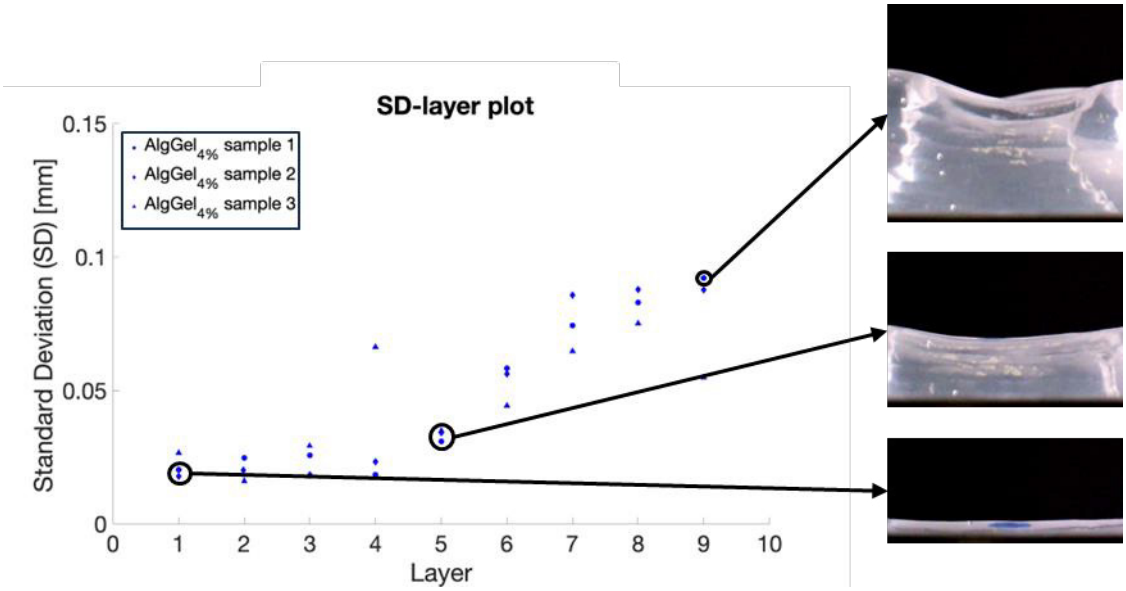

Figure 3. Standard deviation of the profile of each layer.

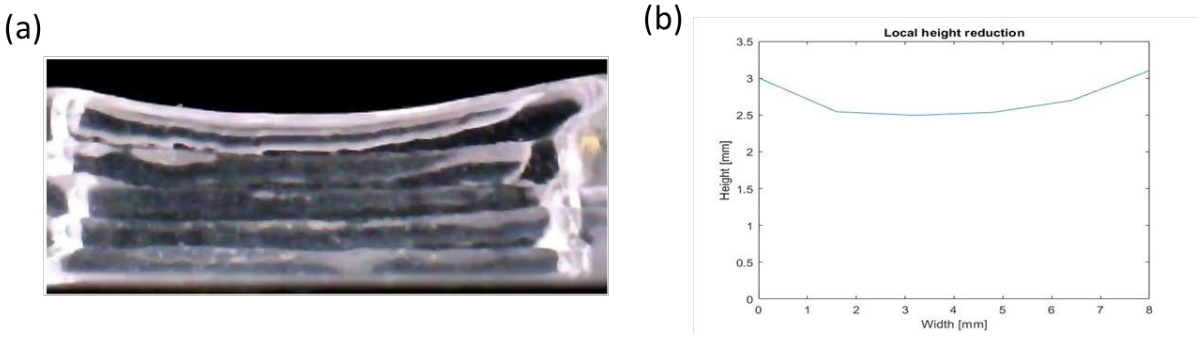

Figure 4. Profile analysis. (a) Original frame grabbed with the digital microscope used for the recordings. (b) Reconstructed profile.

Furthermore, through the height extraction algorithm, it was possible to study the deformation of the structure layer-by-layer. For this purpose, standard deviation (SD) trend was studied as function of layers. In this context, SD was related to the height dispersion along the width of the printed object, thus giving a primary semi-quantitative description of the deformation of its profile. It was observed that for increasing values of SD in subsequent layers, the structure tended to distort, while when SD value remained stable in subsequent layers, the profile of the printed object resulted flatter (Figure 3).

Subsequently, height reduction and deformation of the printed object were studied. The aim of the experiment was to understand if it is possible to study the evolution of the profile of a printed structure from a local point of view. A height matrix was created to store the height information of each column over time. With this approach, it was possible to reconstruct the profile of the printed object and to fully describe its evolution over time (Figure 4).

Peer-review under responsibility of the scientific committee of the 18th CIRP Conference on Intelligent Computation in Manufacturing Engineering, 10-12 July, Gulf of Naples, Italy

4. Discussion

The height reduction phenomenon was measured in every layer deposition, and this behaviour had a non-linear trend over time, which is coherent with the viscoelastic behaviour of soft biomaterials. Furthermore, we could observe that height reduction trend is a function of time which tents to flatten over a constant value. Indeed, in the corresponding videos a rapid height reduction in the first part, and a long slow reduction in the remaining part were observed.

In the profile deformation analysis, it was observed that standard deviation (SD) value had an increasing tendency in subsequent layers in almost all the samples considered. Since SD was used to observe the height distribution along the width of the printed object, its increasing value could be associated to a higher deformation of the object itself. However, in the cases of SD decrease we noticed that a layer was deposited in better way with respect to its previous, flattening the profile of the printed object. From this primary semi-quantitative analysis, we were able to investigate the profile evolution over layers, since a more deformed layer would result in a more uneven distribution of height values along the width of its profile.

To better understand the behaviours of height reduction and profile deformation, subsequent local evaluation was necessary. Observing every single column of each frame and storing the corresponding height value over time allowed us to precisely identify a non-uniformity in height reduction. In fact, studying the printed object profile with respect to different timepoints, it was possible to observe that the profile changed its geometry in a non-uniform way. However, it did not happen in all the samples, and the differences in height reduction between the central part and the extremities was not relevant to be quantitatively determined.

5. Conclusions

The monitoring system proposed in this work allowed us to study the printability of alginate-gelatin-based biomaterials in a novel way. Indeed, our approach allowed us to study a multi-layer structure and to simulate longer printing processes by stopping the extrusion for a certain amount of time. In this way, biomaterial analyses focused on a more realistic condition.

We were able to analyze the height reduction trend over time. Moreover, a preliminary analysis of the profile deformation paves the way to a novel approach for assessing the printability of a biomaterial along the entire printing process.

Thanks to this preliminary result, several directions for further research are foreseen. First of all, we plan to have a more complete description of the effect of the biomaterials, using more bioinks with different monomers concentration, and different biomaterials, in order to evaluate the most suitable one for a specific application. Furthermore, this method could be used in a more detailed analysis of biomaterials printability with respect to the printing parameters used (pressure, velocity, temperature).

In light of these considerations, the development of robust monitoring and control mechanisms for the stand-off distance emerges as a pressing imperative in advancing bioprinting technology. Real-time monitoring techniques, such as optical sensors and computer vision algorithms, offer promising avenues for ensuring precise control and adjustment of the stand-off distance throughout the printing process. By integrating such monitoring capabilities into bioprinting platforms, researchers can enhance printing accuracy, reproducibility, and overall construct quality, thereby unlocking the full potential of bioprinting in tissue engineering and regenerative medicine.

In conclusion, as bioprinting continues to push the boundaries of tissue fabrication with increasingly complex constructs, the meticulous management of the stand-off distance emerges as a critical determinant of printing accuracy, structural integrity, and functional performance. By leveraging advanced monitoring and control strategies, researchers can navigate the challenges posed by extended printing times and intricate geometries, paving the way for the realization of transformative biomedical applications.

Acknowledgements

This study was carried out within the MICS (Made in Italy – Circular and Sustainable) Extended Partnership and received funding from the European Union Next-GeneraFonEUv (PIANO NAZIONALE DI RIPRESA E RESILIENZA (PNRR) – MISSIONE 4 COMPONENTE 2, INVESTIMENTO 1.3 – D.D. 1551.11-10-2022, PE00000004).

References

[1] A. Merin Bejoy *et al.*, “An insight on advances and applications of 3d bioprinting: A review,” pp. 2405–8866, 2021, doi: 10.1016/j.bprint.2021.e00176.

[2] N. Cubo-Mateo, S. Podhajsky, D. Knickmann, K. Slenzka, T. Ghidini, and M. Gelinsky, “Can 3D bioprinting be a key for exploratory missions and human settlements on the moon and mars?,” *Biofabrication*, vol. 12, no. 4, 2020, doi: 10.1088/1758-5090/abb53a.

[3] T. Ghidini, “Regenerative medicine and 3D bioprinting for human space exploration and planet colonisation,” *J Thorac Dis*, vol. 10, no. Suppl 20, pp. S2363–S2375, 2018, doi: 10.21037/jtd.2018.03.19.

[4] T. Ghidini, M. Grasso, J. Gumpinger, A. Makaya, and B. M. Colosimo, “Additive manufacturing in the new space economy: Current achievements and future perspectives,” *Progress in Aerospace Sciences*, vol. 142. Elsevier Ltd, Oct. 01, 2023. doi: 10.1016/j.paerosci.2023.100959.

[5] N. Majumder and S. Ghosh, “3D biofabrication and space: A ‘far-fetched dream’ or a ‘forthcoming reality’?,” *Biotechnol Adv*, vol. 69, p. 108273, Dec. 2023, doi: 10.1016/J.BIOTECHADV.2023.108273.

[6] A. Van Ombergen *et al.*, “3D Bioprinting in Microgravity: Opportunities, Challenges, and Possible Applications in Space,” *Adv Healthc Mater*, vol. 12, no. 23, p. 2300443, Sep. 2023, doi: 10.1002/ADHM.202300443.

[7] X. Guo, D. Wang, B. He, L. Hu, and G. Jiang, “3D Bioprinting of Cultured Meat: A Promising Avenue of Meat Production,” *Food and Bioprocess Technology*.

Springer, 2023. doi: 10.1007/s11947-023-03195-x.
[8] D. H. Kang *et al.*, "Engineered whole cut meat-like tissue by the assembly of cell fibers using tendon-gel integrated bioprinting," *Nat Commun*, vol. 12, no. 1, Dec. 2021, doi: 10.1038/s41467-021-25236-9.
[9] D. Lanzoni *et al.*, "Biotechnological and Technical Challenges Related to Cultured Meat Production," *Applied Sciences 2022, Vol. 12, Page 6771*, vol. 12, no. 13, p. 6771, Jul. 2022, doi: 10.3390/APP12136771.
[10] S. Santoni, S. G. Gugliandolo, M. Sponchioni, D. Moscatelli, and B. M. Colosimo, "3D bioprinting: current status and trends—a guide to the literature and industrial practice," *Biodes Manuf*, vol. 5, no. 1, pp. 14–42, 2022, doi: 10.1007/s42242-021-00165-0.
[11] S. Strauß, R. Meutelet, L. Radosevic, S. Gretzinger, and J. Hubbuch, "Image analysis as PAT-Tool for use in extrusion-based bioprinting," *Bioprinting*, vol. 21, no. November 2020, 2021, doi: 10.1016/j.bprint.2020.e00112.
[12] S. G. Gugliandolo, A. Margarita, S. Santoni, D. Moscatelli, and B. M. Colosimo, "In-situ monitoring of defects in extrusion-based bioprinting processes using visible light imaging," *Procedia CIRP*, vol. 110, no. C, pp. 220–225, 2022, doi: 10.1016/j.procir.2022.06.040.
[13] M. Uzun-Per *et al.*, "Automated Image Analysis Methodologies to Compute Bioink Printability," *Adv Eng Mater*, vol. 23, no. 4, pp. 1–12, 2021, doi: 10.1002/adem.202000900.
[14] Z. Jin, Z. Zhang, X. Shao, and G. X. Gu, "Monitoring Anomalies in 3D Bioprinting with Deep Neural Networks," *ACS Biomater Sci Eng*, 2021, doi: 10.1021/ACSBIOMATERIALS.0C01761.
[15] S. Yang, L. Wang, Q. Chen, and M. Xu, "In situ process monitoring and automated multi-parameter evaluation using optical coherence tomography during extrusion-based bioprinting," *Addit Manuf*, vol. 47, p. 102251, 2021, doi: 10.1016/j.addma.2021.102251.
[16] L. Wang, M. E. Xu, L. Luo, Y. Zhou, and P. Si, "Iterative feedback bio-printing-derived cell-laden hydrogel scaffolds with optimal geometrical fidelity and cellular controllability," *Sci Rep*, vol. 8, no. 1, pp. 1–13, 2018, doi: 10.1038/s41598-018-21274-4.
[17] A. A. Armstrong, A. Pfeil, A. G. Alleyne, and A. J. Wagoner Johnson, "Process monitoring and control strategies in extrusion-based bioprinting to fabricate spatially graded structures," *Bioprinting*, vol. 21, no. September 2020, p. e00126, 2021, doi: 10.1016/j.bprint.2020.e00126.
[18] Gugliandolo Simone Giovanni, Prioglio Egon, Moscatelli Davide, and Colosimo Bianca Maria, "A new solution for in-situ monitoring of shape fidelity in extrusion-based bioprinting via thermal imaging," 2024.
[19] M. Ogunsanya, J. Isichei, S. K. Parupelli, S. Desai, and Y. Cai, "In-situ droplet monitoring of inkjet 3D printing process using image analysis and machine learning models," *Procedia Manuf*, vol. 53, pp. 427–434, 2021, doi: 10.1016/j.promfg.2021.06.045.
[20] B. T. Lies, Y. Cai, E. Spahr, K. Lin, and H. Qin, "Machine vision assisted micro-filament detection for real-time monitoring of electrohydrodynamic inkjet printing," *Procedia Manuf*, vol. 26, pp. 29–39, 2018, doi: 10.1016/j.promfg.2018.07.004.
[21] K. K. Moncal, V. Ozbolat, P. Datta, D. N. Heo, and I. T. Ozbolat, "Thermally-controlled extrusion-based bioprinting of collagen," *J Mater Sci Mater Med*, vol. 30, no. 5, 2019, doi: 10.1007/s10856-019-6258-2.